

Article

Design and Implementation of Automatic Cooling Case Based on High-Power and High-Density Power Supply Array

Zerui Chen ^{1,*} , Hangwei Feng ² , Guoguang Zhang ¹ and Chong Yang ¹

¹ Kunming Shipbuilding Equipment Research and Test Center, Kunming 650051, China; rsw1986@mail.nwpu.edu.cn (G.Z.); e_yangchong@163.com (C.Y.)

² The 54th Research Institute of CETC, Shijiazhuang 050081, China; fenghw@dsp.ac.cn

* Correspondence: xiaoruibest@yeah.net

Abstract: Multi-board electronic cases with high-density and power modules are widely used in industrial power supply management. Heat dissipation becomes an important factor in the design process in improving case performance and miniaturization requirements. The design of existing small electronic thermal methods ignores high-temperature and high-load environment tests without automation control. To solve these problems, a heat dissipation case is designed with a magnesium and aluminum alloy, for intelligent temperature control based on a high-power and high-density power supply array. Based on the extreme miniaturization design principle, a composite heat dissipation mode is adopted based on conduction and supplemented by forced air cooling. The results show that the heat dissipation design in this article can work normally in high-temperature and high-load environment tests. Finally, the existing cooling designs are compared and analyzed. The cooling performance parameters in this article are better than those in the existing case. It contributes to the thermal design of miniaturized electronic cases in power supply management.

Keywords: thermal design; miniaturization; high power; high density; automation



Citation: Chen, Z.R.; Feng, H.W.; Zhang, G.G.; Yang, C. Design and Implementation of Automatic Cooling Case Based on High-Power and High-Density Power Supply Array. *Electronics* **2023**, *12*, 4353. <https://doi.org/10.3390/electronics12204353>

Academic Editors: Hongchang Li and Jingyang Fang

Received: 13 September 2023

Revised: 16 October 2023

Accepted: 17 October 2023

Published: 20 October 2023



Copyright: © 2023 by the authors. Licensee MDPI, Basel, Switzerland. This article is an open access article distributed under the terms and conditions of the Creative Commons Attribution (CC BY) license (<https://creativecommons.org/licenses/by/4.0/>).

1. Introduction

In recent years, due to the increasing requirements for miniaturization and lightweight industrial products, power arrays are developing in the high-density, high-power, and intelligent directions [1]. Temperature rise is a critical factor affecting the reliability of power modules. With an increase in temperature, the failure efficiency of electronic components shows an exponential growth trend, which seriously affects the regular operation of supply load [2]. With the increase in working hours, some cooling measures must be taken to limit the temperature rise in clustered power modules.

Frequently used thermal design methods include physical structure heat dissipation and modeling optimization heat dissipation. Physical structure heat dissipation can be divided into natural air cooling, conduction cooling, forced air cooling, circulating water cooling, and so on. Natural air cooling mainly transfers heat from the power module shell to the air through natural convection or conducts it to the PCB through pins. The conductive heat dissipation includes a layer of heat-conducting silicone sheet and resin between the shell and the module, so that the body and the module are closely combined. Forced air cooling provides for the use of fans to increase airflow to remove accumulated heat. Circulating water cooling involves placing water-filled conduits on top of the heat module to dissipate heat through flow liquor. Software modeling mainly uses computers to conduct thermal simulation calculations with environmental parameters, including structural heat dissipation characteristics and heat source layout. It guides the relevant thermal design after establishing thermal simulation models.

To solve the problem of heat dissipation of power arrays, various researchers adopt single or combined physical methods based on general thermal design measures and

use software analysis. They fail to solve the problem of heat dissipation fundamentally, comprehensively, systematically, and entirely and may find new issues or risks when translated. The paper [3] combines methods (natural air cooling, thermal conduction, forced air cooling) used for heat dissipation. The optimized structure can meet the heat dissipation requirements, but the selected test power supply has low power and still needs to meet the design requirements of high strength and high density. In addition, the numerical simulation method does not consider the influence of materials on conduction heat. The paper [4] adopts a forced air cooling method and establishes a three-dimensional simulation model. The heat dissipation conditions are improved by optimizing the air intake channel. However, all the simulation data remain in the theoretical calculation stage, and the actual heat dissipation effect needs complete test verification. The paper [5] designs an air–liquid water-cooling cabinet and optimizes the structural size design. The heat dissipation effect is improved due to the optimization of the structure layout, but the heat exchange improves the power consumption of the whole system. If the cold plate is subjected to severe impact, vibration, and extrusion, it may lead to leakage of coolant, threatening the safety of the whole system. It can be seen that the current thermal design scheme has more or less the following problems. Firstly, only from the perspective of the heat dissipation channel, heat dissipation layout, and software modeling, the heat dissipation environment is optimized to improve the heat dissipation effect, whereas the efficiency of the heat source, the use of conductive materials, and other factors are not considered. Secondly, the effectiveness of thermal design measures can only be verified with high load tests based on miniaturization, high power, and a high-density design. Thirdly, the software modeling environment is ideal, and the simulation parameters are straightforward. A lack of test data results in a specific deviation between the simulation environment and the natural environment with load, which is insufficient to guide the thermal design further. Fourthly, improving the heat dissipation performance results in reliability degradation of the system. Fifthly, the lack of logic for monitoring temperature, current, and voltage-related operation data of heat source devices and the formation of feedback regulation may lead to excessive thermal design. For example, forced air cooling can cause an improvement in static power consumption, resulting in unnecessary operation noise.

In this paper, a highly miniaturized high-power and high-density power array is designed. High-efficiency DC/DC modules are selected as the heating source. Magnesium and aluminum alloys are used as the primary structural materials in heat dissipation, and graphene is the conduction material between the heat source and the cold plate. They can ensure that the power array case has high thermal conductivity while considering high strength, lightweight, and anti-electromagnetic interference characteristics. Natural air cooling and conduction heat dissipation are combined, and forced air cooling is a supplement. In addition, the MCU chip, multi-point temperature, voltage, and current sensors, A/D acquisition chip, relay, and other automation modules can intelligently monitor the temperature rise of each point of the power module and then control the power array and forced air cooling starting time. Finally, the electronic case is placed for testing in a closed thermal environment for dynamic loading. The results show that the heat dissipation system can effectively improve the heat dissipation condition and reduce the working temperature of the whole system without sacrificing the performance and can meet the requirements of fast response and continuous and efficient output power of the power array. The output power of the entire system is not less than 10,000 W, and the lowest packing-level density is not less than 47 W/cm² with high reliability, portability, and practicability. It also provides technical and prototype support for the standardized design of similar power arrays.

The paper is structured as follows. Section 2 presents the thermal design methods of heat dissipation of physical form and heat dissipation optimization by modeling. Section 3 offers the design of an automatic cooling case based on a high-power power supply array, including conduction cooling design, forced air cooling design, high power density

power supply array design, and automatic control module design. Section 4 analyzes and compares the test results with related performance parameters. Section 5 discusses the experimental conclusions and future research.

2. Related Works

In recent years, various research teams have proposed solutions to the heat dissipation problem of closed power supply cases (modules) with high power density and small volumes from different perspectives, which can be roughly divided into two categories as in Table 1: physical structure heat dissipation and modeling optimization heat dissipation.

Table 1. Heat dissipation solution.

Classification	Solutions	Reference
Physical structure heat dissipation	natural air cooling	[3]
	conduction cooling	[3]
	forced air cooling	[4]
	circulating water cooling	[5]
Modeling optimization heat dissipation	Thermodynamic analysis software	[5]

The heat dissipation of physical structures is usually improved or optimized by combining natural air cooling, conduction cooling, forced air cooling, and circulating water cooling. Li [3] analyzes the heat dissipation path of a high power density closed power supply and proposes a design method to strengthen heat dissipation by using the shell extension surface structure of a rectangular fin to increase the conduction refrigeration area. Yu [6] adopts heat pipe cooling technology in cold plates to improve the heat transfer capacity of hard scale. Fu [7] designs the structure and method of ventilation and heat dissipation of a new energy storage power supply, which realizes uniform heat dissipation inside the energy storage power supply through such structures and processes it through the air inlet and air guide plate at the bottom of the energy storage power supply, switchable cooling mode, and independent air duct outlet. Tan [4], aiming at the heat dissipation problem of the power cabinet of airborne equipment, adopts the method of forced air cooling to reasonably improve the air intake pipe to reduce the pressure loss in the line and achieve better air cooling heat dissipation effects. Ben [2] adopts the distributed forced air cooling for heat dissipation of the modular DC power cabinet in the substation, which effectively controls the temperature difference between the power module and the radiator. However, these solutions are based on the physical heat dissipation of the selected power module's combination power density, which is low, and only use the heat dissipation structure to optimize adjustment. Without using a closed extreme environment for a long time with a load output test, the cooling effect is unknown, so there is no fundamental solution to the problem of heat dissipation. In addition, structural adjustment may bring low reliability of the whole system.

Thermodynamic analysis software is usually used to establish the simulation model of the power supply, which is used to verify the technical requirements and optimize the product structure and selection design to provide practical and rigorous design scheme guidance for the air-cooled or water-cooled cabinets used in the industrial field. Yang [5] conducts a three-dimensional simulation analysis of the whole machine to understand the local cooling air path design, the gas-liquid heat exchange device, and the corresponding cold plate for the ship-borne, water-cooled cabinet, and also conducts a heat simulation to check the cooling effect and optimize the structural design. Zhang [8] calculates the influence of the outlet pressure of the switching power supply on the wind speed of the fan inside the switching power supply and the impact of the inlet wind speed of the power supply on the temperature of the heat source inside the power supply by theoretical calculation

and numerical simulation, verifies the rationality of the heat dissipation characteristics and structural design of the model, and provides valuable data for the configuration, simulation, optimization, and application of related equipment. Huang [9] uses mathematical modeling and finite element analysis methods. ANSYS simulation analysis software is used to analyze the heat dissipation structure of a high-power microwave power supply and proposes structural optimization measures for cooling water flow, fan inlet flow, and fin thickness. Niu [10] establishes the thermal resistance model of the power module. By analyzing the coupling relationship between the primary heat sources, the temperature rise was calculated, and the thermal simulation model was established by Flotherm software to verify the correctness of the thermal resistance model. Given the thermal stress concentration point, the thermal performance optimization design scheme was proposed. However, these software-based modeling solutions only stay in the ideal simulation stage; the thermal conductivity of heat dissipation materials, power module characteristics, room temperature changes, and other factors are not included in the simulation model, resulting in a large gap between the model and the actual application scenario. The ultimate purpose of simulation is only to improve the heat dissipation structure, not to fundamentally solve the heat dissipation problem. Secondly, other thermal simulation models also verify the simulation model of thermal resistance. Therefore, there is no support for and verification of actual data for the model's validity.

3. Design of an Automatic Cooling Case

The automatic heat dissipation case mainly follows the principle of heat source suppression and heat dissipation environment improvement. Firstly, it reduces thermal power from the selection and design of heat sources. Secondly, it improves the heat dissipation environment by optimizing the conduction and air-cooling heat dissipation as a supplement. Configuration of the automatic cooling case includes: conduction heat dissipation design, forced air cooling design, high-power density power supply array design, and mechanical control module design.

3.1. Conduction Heat Dissipation Design

3.1.1. Selection of Conductive Heat Dissipation Materials

In conductive heat dissipation, the methods to reduce thermal resistance include replacing high thermal conductivity materials and increasing the area of the heat dissipation structure [11]. Metals are commonly used as heat-dissipating materials in industrial products. Magnesium–aluminum alloy is an aluminum alloy with Mg as the main added element. Magnesium metal has the most negligible density of the widely used metals; magnesium ($\rho = 1.8 \text{ g/cm}^3$) alloy is 20% lighter than plastic and 30% lighter than aluminum. The strength and quality of magnesium alloy are high, and it has a specific bearing capacity. Its heat conductivity is 100 times that of PP material. Related studies have shown that cooling speed is related to parameters (ρ and c) of the materials' density and heat capacity. Material heat capacity parameters (ρ and c) are determined by the type of material, which significantly influences the cooling speed at the beginning of the cooling. Magnesium alloy AZ91D, for example, compared with aluminum alloy, has its values of ρ (1.8) and c (1.02) as fixed and low, so it has a faster speed of reduction of temperature in the air [12]. Therefore, magnesium–aluminum alloy has high thermal conductivity with lightweight and high strength characteristics, making it the best choice for cold plate and chassis materials. Furthermore, graphene has recently been advocated for high-power thermal management enhancement in non-metallic materials, such as heat dissipation in high-density integrated circuits, due to its high thermal conductivity of 5300 W/MK. Packaging composites with high thermal conductivity can be prepared by filling graphene into the polymer matrix, which is much better than other fillers [13].

3.1.2. Structure Design of Conduction Heat Dissipation

This paper uses the finned AZ91D magnesium–aluminum alloy cold plate structure to increase the heat dissipation area. Graphene is the heat conduction material between the cold plate and the DC/DC module. Figure 1 shows a side view of the conduction heat dissipation structure. Figure 2 shows the top view of the conduction heat dissipation structure. In Figure 2, the covered part of the cold plate is gray, and the DC/DC power supply is red. The cold plate opening is white, and the graphene heat sink area is dotted black. The heat conduction and heat dissipation channel is: DC/DC module interior → module shell → graphene → magnesium–aluminum alloy cold plate surface → fin structure → internal case environment.

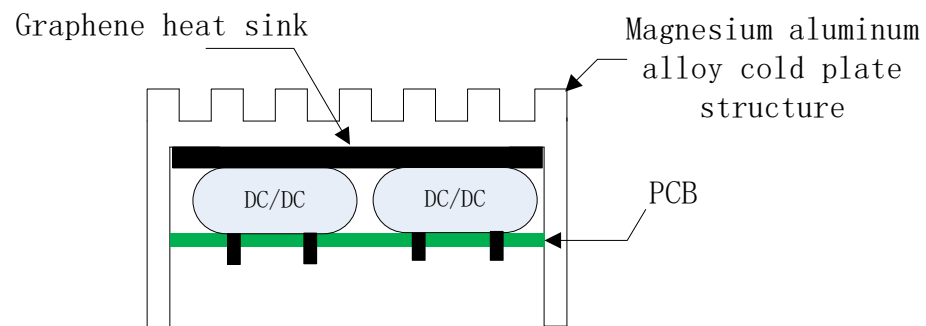


Figure 1. Side view of conduction heat dissipation structure.

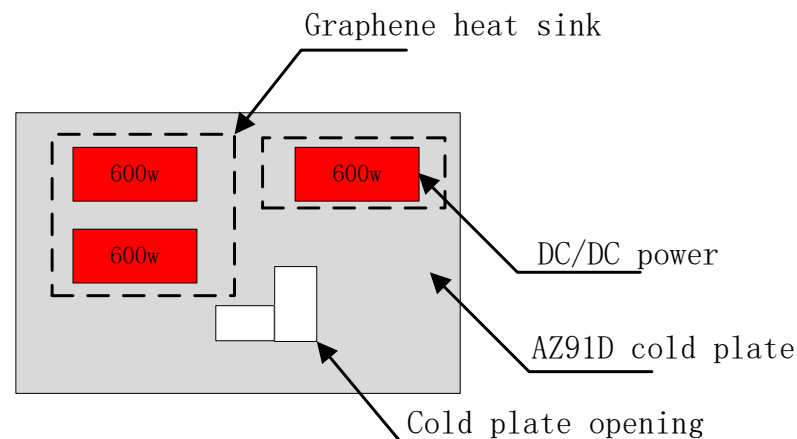


Figure 2. Top view of conduction heat dissipation structure.

Two PCB boards load each series of the power supply. Taking the DCM3714 series as an example, the three-dimensional structure diagram of one panel is shown in Figure 3. The power array consists of six power array PCBs and a control PCB, and the final schematic diagram of the heat dissipation structure of the electronic case is shown in Figure 4. The container size is about $28.1 \times 23.8 \times 15.9$ (cm³), which meets the requirements of miniaturization design [14]. As shown in Figure 4, the guide rail design on both sides not only serves to install the structure of the electronic chassis mechanically but also acts to transfer the heat from the surface of the case to the external mounting structure. As shown in Figure 5, the contactor and filter capacitor are installed at the bottom of the case. The contactor controls 300 V high-voltage input power, and the filter capacitor filters the ripple of the high-voltage input. Figure 6 shows the schematic diagram of the overall heat dissipation structure after the panel is assembled on the case.

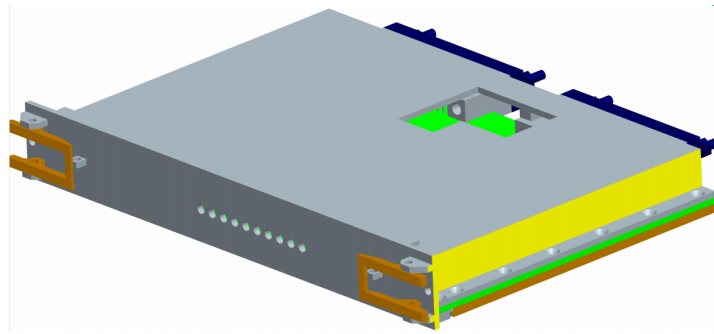


Figure 3. Three-dimensional diagram of PCB.

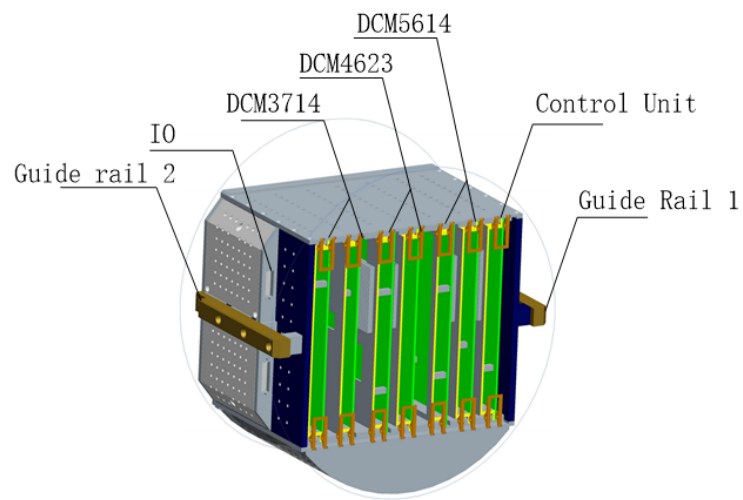


Figure 4. Cutaway view of dissipation structure of electronic case.

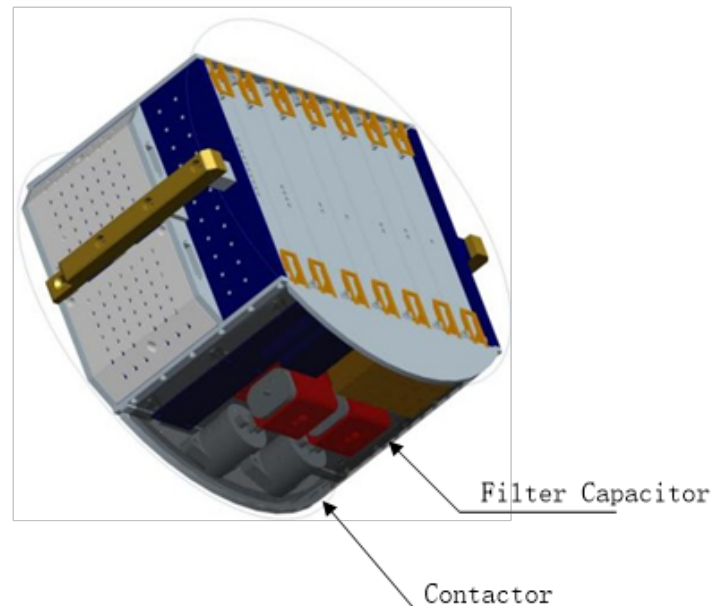


Figure 5. Schematic diagram of the bottom of the electronic case.

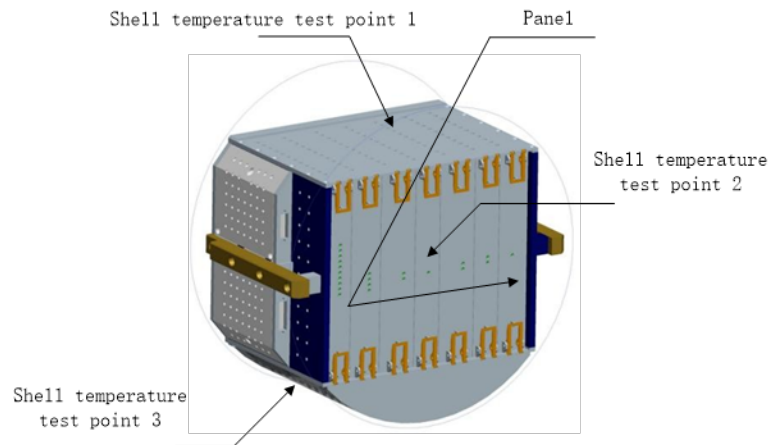


Figure 6. Schematic diagram of the overall heat dissipation.

The thermal conductivity in the PCB thickness direction (i.e., vertical direction) is much smaller than in the plane direction. To improve the thermal conductivity in the thickness direction, the heat dissipation hole can be designed directly below the bottom of the heating source. According to the optimization theory of the heat dissipation hole [15], a 0.045 cm diameter of the inner cavity of the heat dissipation hole is the optimal diameter, and the thermal conductivity can be increased by about 6.5%. Filling with a material with high thermal conductivity, such as solder, can increase thermal conductivity by about 35%.

As shown in Figure 7, the aperture of PCB in this paper is set to 0.045 cm. The method of treating the hole with oil, which is conventional in PCB treatment technology in the production process, can be adopted, and the hole spacing is kept at 1 mm. The hole from DC/DC soldering is used to fix the DC/DC module. To further increase the heat dissipation effect, all the holes are covered with copper (the red part in Figure 7). The advantages of the copper part are that it can increase the heat dissipation area and form a large ground layer, or power layer, which can reduce electromagnetic interference and circuit noise.

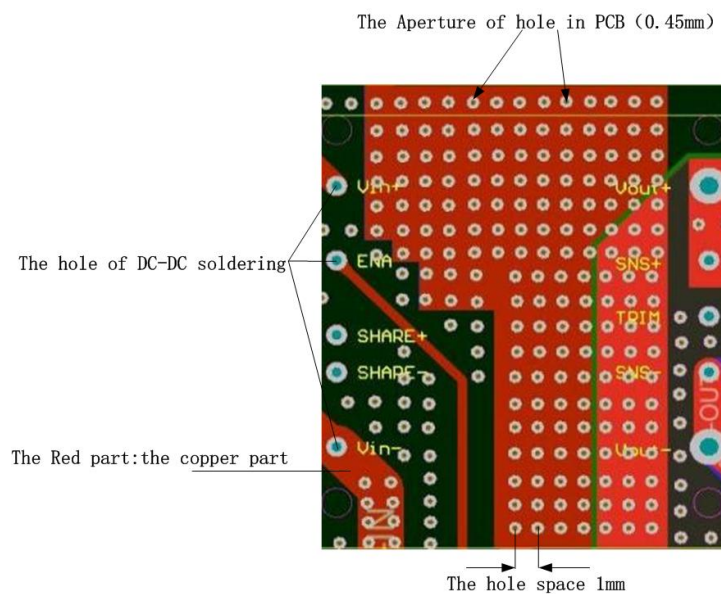


Figure 7. PCB copper-covered heat sink.

According to the convection heat transfer formula [16]:

$$Q = h_c A (t_m - t_f), \tag{1}$$

where h_c indicates heat flow rate through the unit area under the action of the unit temperature difference and is defined as convective heat transfer coefficient ($W/cm^2 \cdot ^\circ C$); A is the heat transfer area (cm^2); t_m is the surface temperature ($^\circ C$); and t_f is the temperature of cooling gas ($^\circ C$). To change the heat dissipation performance of the case, the convective heat transfer coefficient or the heat transfer area can be changed, and the area of the heat dissipation hole directly represents the heat transfer area. Therefore, the layout of the heat dissipation hole and the opening rate of the heat dissipation hole become important factors in heat dissipation efficiency. To enhance the heat dissipation effect of natural and forced air cooling, the heat inside the electronic case is transferred to the outside promptly while considering electromagnetic compatibility and aesthetic design principles. Mechanical circular holes are designed around the case (at the bottom and the top) to expand the heat dissipation channels. The diameter of the circular holes is set to 2 mm, and the gap between the holes is set to 5 mm, as shown in Figure 8.

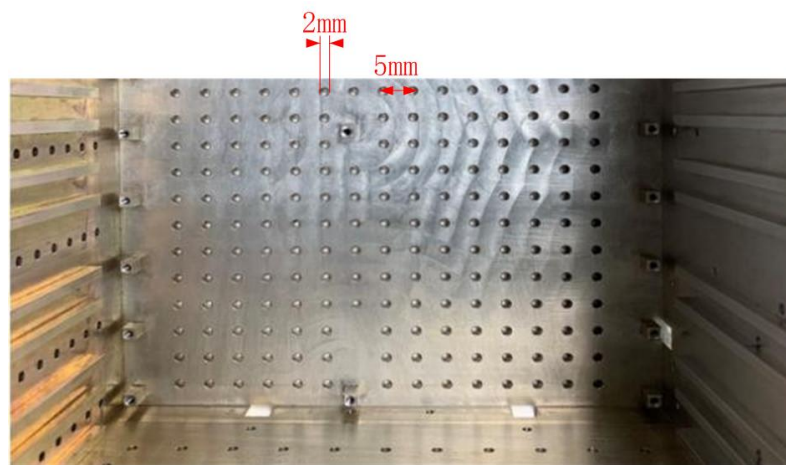


Figure 8. Heat emission hole of the electronic case.

3.2. The Design of Forced Air Cooling

Forced air cooling is usually more effective than thermal conduction, and the commonly used forced air cooling method is mainly composed of fans. Under the condition of satisfying the air volume, fans with high air pressure should be selected as much as possible. The structure of the cooling air duct should avoid a 90° bending angle to ensure that the heat generated by the switching power supply can be dissipated in time [9]. The fan design in this paper is independent of the electronic case and is placed at the top and bottom of the case at a distance of about 5 cm. The angle of the cooling air duct is designed to be 0° . The heat trend diagram is roughly shown as the arrow in Figure 9. The installation inside the case takes up considerable space, which helps to reduce the size of the electronic case. Introducing fans will inevitably increase the power consumption and noise of the system, and the reliability will be reduced to varying degrees. Therefore, if the average operating temperature is not higher than the preset shell temperature, only conduction heat dissipation is used in this paper. The heat transfer and heat dissipation channels of forced air cooling are as follows: DC/DC module interior \rightarrow module shell \rightarrow graphene \rightarrow surface of Mg–Al alloy cold plate \rightarrow fin structure \rightarrow internal environment of the chassis \rightarrow Mg–Al alloy surface of the case \rightarrow external environment of the case. From the direction of heat dissipation, it can be seen that forced air cooling is only conducive to speeding up the effect of conduction heat dissipation. Therefore, the overall cooling effect mainly depends on thermal conduction.

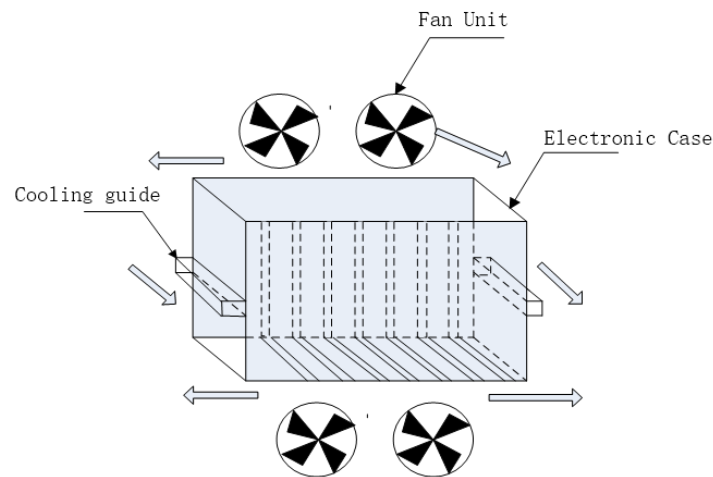


Figure 9. Schematic diagram of forced air cooling of the electronic case.

3.3. The Design of High-Power Density Power Array

The efficiency of DC/DC determines the thermal power consumption, and the thermal power consumption determines the operating temperature [5]. Therefore, selecting highly efficient DC/DC helps reduce the caloric value from the heat source. The theoretical formula of thermal power consumption is shown as follows [6]:

$$P = P_0(1 - Y) / (Y). \tag{2}$$

P is the thermal power. P_0 is the inherent output power of the DC/DC module. Y is the efficiency of DC/DC output at full load. $(1 - Y) / Y$ is the thermal power coefficient. The thermal power coefficient determines the heating power when the inherent output power is unchanged. Table 2 shows the corresponding relationship between DC/DC full-load output efficiency and thermal power consumption coefficient. It can be seen from the table that the higher the efficiency, the lower the thermal power consumption coefficient. With every 1% increase in efficiency, the temperature rise per time unit can be reduced by at least 5%. When the efficiency is increased by about 10%, the thermal power consumption can be significantly reduced by about 69% compared with the initial state. Therefore, improving efficiency is more effective than optimizing the heat dissipation channel or structure.

Therefore, according to the relationship between DC/DC efficiency and thermal power consumption coefficient (as shown in Table 2), the DCM Chip series power supply of the VICOR Company is mainly selected to form the power array (as shown in Table 3). It is an isolated DC/DC converter with stabilized voltage, which can run in a wide range of unstabilized voltage inputs to generate isolated output. Efficiency can be up to 96% (output power greater than 90% of the design power), and power density can be up to 75.9 W/cm^3 , with the characteristics of input under-voltage protection, output over-voltage, over-current, short circuit protection, and over-temperature protection.

Table 2. DC/DC efficiency and thermal power consumption coefficient.

DC/DC Efficiency at Full Load Output	Thermal Consumption Coefficient
86%	0.16
89%	0.12
90%	0.11
92%	0.09
95%	0.05

Table 3. DC/DC series power supply information.

N	DC/DC	Maximum Power	Efficiency	Power Density	Number	Input	Output	Heat Density
1	DCM3714	600 W	94.0%	18.9 W/cm ³	6	200–420 V	12–28 V	116 W/cm ²
2	DCM4623	500 W	92.8%	63.5 W/cm ³	6	160–420 V	12–28 V	47 W/cm ²
3	DCM5614	1300 W	96.0%	27.5 W/cm ³	4	180–400 V	22–36 V	166 W/cm ²

Total power $\geq 10,000$ W. DC/DC average power density ≥ 36.6 W/cm³. Electronic case power density ≥ 1000 W/cm³.

DC/DC power density [16] is defined as:

$$P_p = P_T / S(V). \quad (3)$$

P_p represents DC/DC power density (W/cm³). P_T indicates the maximum output power of DC/DC (W). $S(V)$ represents the surface area or volume (cm²) of the DC/DC orthographic projection. However, the current definition of power density in the design of small electronic cases only depends on evaluating a single DC/DC module. When several DC/DCs are used to form a power array to form a systematic design, the power density of a single module cannot represent the power density of the whole system. In addition, the actual output power is far from the maximum output power, resulting in a higher power density. In this paper, a three-dimensional case power density is defined, which can reflect the thermal design index of the electronic case more comprehensively:

$$P_V = (\sum P_i) * N / V_m. \quad (4)$$

P_V indicates the power density of the electronic case (W/cm³). P_i means the maximum output power (W) of all DC/DC modules in the case. N shows the actual power output percentage (%). V_m stands for the volume of the design case cavity (not including the thickness of the case) (cm³). For large electrical equipment, the power may be more than 3000–5000 W. If a high power supply's overall design and packaging are used, applying the device stress will be extensive. The corresponding volume and cost will be multiplied. Suppose multiple low-power power sources are used to achieve high-power output (such as three power sources (1000 W) in parallel to achieve 3000 W output power). In that case, the difficulty of the design will obviously be reduced. Meanwhile, from the system's perspective, saving costs and improving reliability are beneficial. To realize the parallel output of power modules, a similar current-sharing technology is usually adopted [17]. In this paper, each DC/DC series adopts the design of equal current-sharing (as shown in Figure 10). The input end is added with a fuse tube, and several 3714/4623/5614 DC/DCs are connected in parallel. Each output end is associated with a diode (to prevent the load voltage recoil-back to protect the power module) combined with electronic load 1–3. Finally, the maximum power output is increased to 3600 W. When any DC/DC fails at high temperature or needs to be cooled temporarily, the current of this module decreases. However, the current of other DC/DC modules increases to compensate for the power loss and ensure the regular operation of back-end loads. Using parallel current sharing technology, the power array designed in this paper contains 16 DC/DC modules, and the total power can reach 10,000 W under a 90% load test. The average power density of DC/DC is higher than 36.61/cm³, and the average power density of the electronic case is up to 61.10 W/cm³.

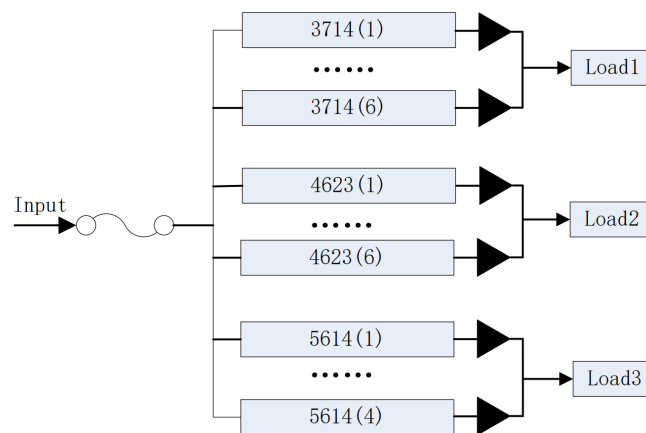


Figure 10. Parallel current equalizing output mode.

3.4. Design of Automatic Control Components

3.4.1. Design of the Automatic Control Module

The automatic control system mainly includes sensor sampling and relay control modules. The relationship between the two is shown in Figure 11. Each IO corresponds to a DC/DC shell temperature test point or shell temperature test point on the surface of the case. An MCU communication link is built between the two modules. When the relay control module detects a high-level signal sent by the sensor sampling module, the MCU1 control mechanism in the relay control module will be triggered.

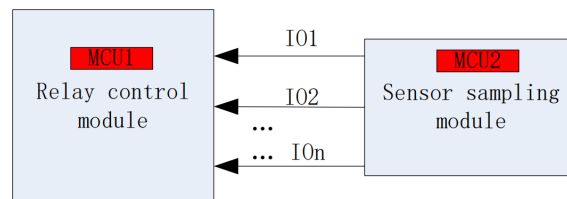


Figure 11. Automatic control system.

The sensor sampling module is shown in Figure 12. The sensor module mainly adopts several temperature, voltage, and current sensors to collect the three analog quantities of the single DC/DC module in each series. The temperature sensor is DS18B20, a single-bus digital temperature sensor from Dallas, USA. The temperature measurement range is -55 – 125 °C, and the temperature value of the analog can be converted and expressed with the resolution of 9, 10, 11, and 12 bits. The unit temperature values corresponding to the above four resolutions are 0.5, 0.25, 0.125, and 0.0625 °C [18]. It can overcome the shortcomings of the traditional control mode and realize accurate, fast, and reliable temperature acquisition and control. In this paper, 9-bit resolution (with a corresponding temperature value of 0.5°) is used for temperature sampling, and the analog quantity is converted into a digital portion using an AD7606 sampling chip to access MCU. The sampling chip is an A/D conversion chip called AD7606, which the American Analog Device Company launched. The high-performance ADC has high resolution, low power consumption, and synchronous sampling characteristics. Among them, two CONVST pins give the chip the advantage of eight-channel synchronous sampling. Meanwhile, the chip integrates an anti-aliasing filter, a high-speed serial, parallel interface, and other modules, making the design of the data acquisition system easier [19]. Each group of sampling chips includes two AD7606 chips. The final sampling and detection results are stored in SPI FLASH for easy viewing.

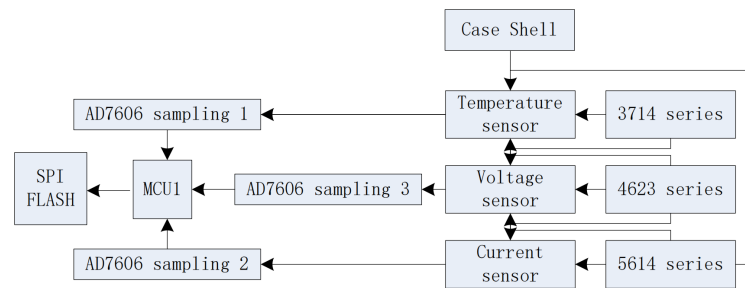


Figure 12. Sensor sampling module.

The application of a relay plays an essential role in the era of automation. It mainly performs a function similar to a switch to protect the operation of electrical appliances and the safety of the line. According to the classification standard of the relay, it can be divided into solid state relay, electromagnetic relay, and thermal relay. When the temperature of the relay is too high, the metal sheet will be heated and appear bent, resulting in low reliability [20]. Because the relay in this paper is mainly used in high-temperature confined spaces, the combination control mode of single-point solid-state relay and multi-point electromagnetic relay is adopted, as shown in Figure 13. The specific control process is as follows: MCU gives a high-level signal to the IO port to drive the solid-state relay, triggering the electromagnetic relay, enabling and controlling a DC/DC or fan in the power module to finish startup and shutdown.

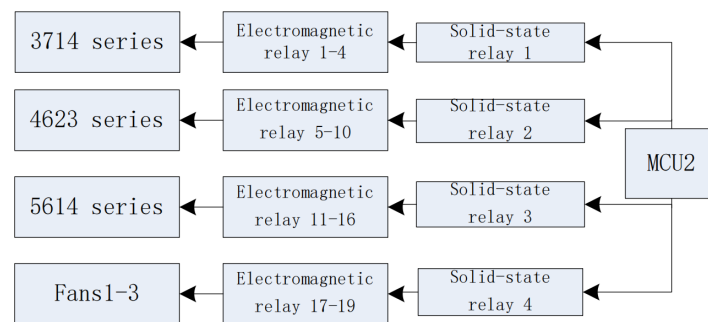


Figure 13. Relay control module.

3.4.2. Design of Automatic Control Software

Generally, it is recommended that the shell temperature of a power module be 10–15° lower than the highest shell temperature, and the highest shell temperature of a DC/DC module is 100°. Therefore, the recommended operating temperature of a single DC/DC module should be controlled within the range of 90°. The temperature test point of a 1–3 shell should be held within 85°, and the maximum temperature value should not exceed 90°. In the design of forced air cooling mode, the heat dissipation capacity of the fan is often positively correlated with the speed of the blade. When the rate cannot be connected with the heat dissipation demand, resulting in the fan set and heat dissipation demand being two unrelated systems, they cannot achieve synchronization [21]. Therefore, in this paper, the speed of the fan bank is set according to the temperature of the test shell. Meanwhile, the rate is set to three levels (low, medium, and high) to avoid energy waste. Low, medium, and high correspond to 0–30%, 30–60%, and 60–100% load power consumption, respectively. According to the sampled data (temperature, voltage, and current of the monitoring point are obtained every 500 ms and stored in the SPI FLASH), the MCU1 determines the critical value. Of vital importance, the MCU1 controls the start and close of the DC/DC module or fan group. The essential significance of a single DC/DC startup/shutdown is shell temperature 90°; power feedback flag bit 1 (if the load power consumption is lower than 30%, MCU enables one-third of the DC/DC output. When the load power consumption is 30% to 60%, MCU enables two-thirds of the DC/DC output; when the load power

consumption is more significant than 60%, MCU allows all DC to DCs output); no voltage output; and abrupt current. The critical value of the shell temperature test points 1–3 is 85°. Startup flag bit 1 indicates that the DC/DC module is enabled, and 0 indicates that the DC/DC module is disabled. Detailed control logic is shown in Figure 14 below.

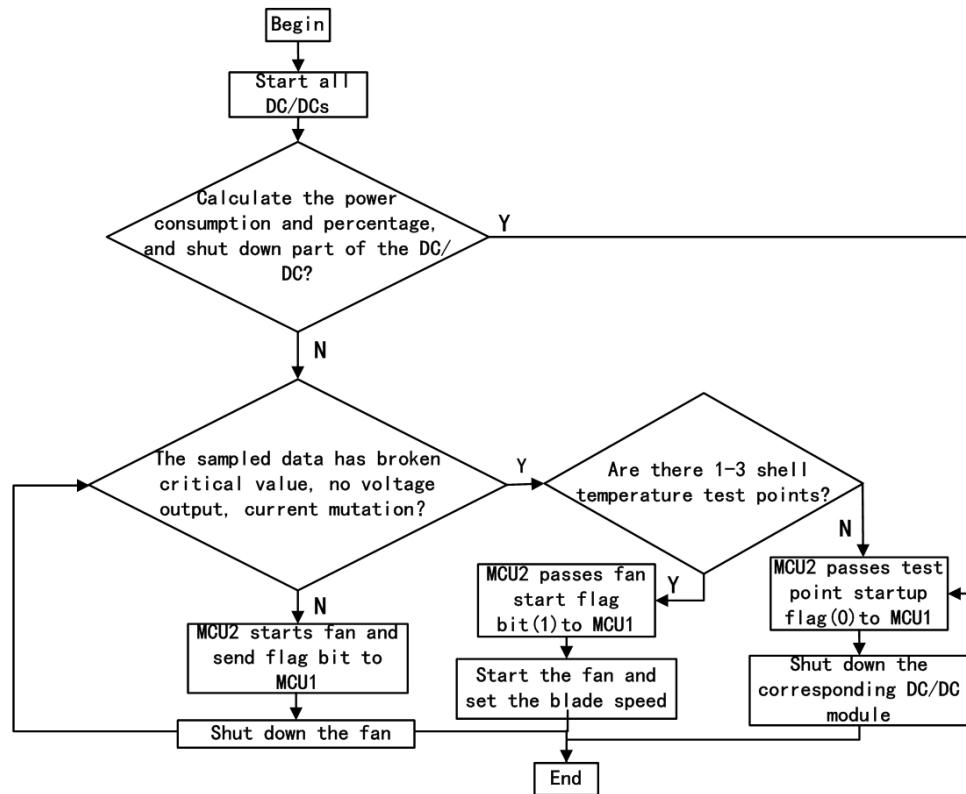


Figure 14. Control logic flow chart.

4. Analysis of Test Results and Comparison of Related Performance Parameters

The test equipment is shown in Table 4.

Table 4. Related test equipment and functions.

Equipment	Function
Power array	Test source
Several 300 V high-voltage power supplies	Supply array power
Electronic loads	Test the performance of the power arrays
Temperature, voltage, current sensors	Monitor running data of the power array
Several multimeters	Monitor DC/DC abnormal data
Automatic control module and control DC/DC startup and shutdown	

4.1. Analysis of Test Results

The electronic load is placed at the output end of the DCM3714, 4623, and 5614 series power supplies, respectively, for the on-load test of the power array. In addition to the DC/DC surface, the detection points of the shell temperature sensor are also placed at the center, top, and bottom of the end cover of the panel of the electronic case, as shown in Figure 6, and defined as shell temperature test points 1–3. The environmental temperature of the test was 0°, 25°, and 40°, and the test altitude was 2000 m. The absorbed power of the electronic load was set as 30%, 60%, and 90% of maximum capacity. All the converters (power supply DCM) will be activated simultaneously at various powers and work at their overall strength. The output power of every DCM will be set as the percentage of the

electronic test load power. Shell temperature test point 2 is located at the center cover of the panel and is close to DC/DC; it can be closer to the shell temperature during DC/DC operation. Therefore, the sensor reads shell temperature test point 2 (the integral part of the temperature is taken for the convenience of analysis) as the maximum temperature point of the electronic case surface so that indexes are analyzed and line diagrams can be drawn.

The relationship between the single output power of DCM and the test percentage of the electronic load power is shown as follows:

$$P_{out} = P_{er} * P_{maxdcm} \tag{5}$$

P_{out} is the output power of a single DCM. P_{er} is the electronic test load power percentage. P_{maxdcm} is the maximum power of DCM and depends on the type of the single DCM, such as DCM3714 (600 W), DCM3714 (500 W), or DCM5614 (1300 W).

The changing trend of temperature over time can be seen in Figures 15 and 16. Under different ambient temperature conditions, the temperature of each curve increases with time. After 120 min of load test, the temperature of shell temperature test point 2 was effectively controlled within the safe range of 85°. By reading the data monitored by the voltage and current sensors in SPI FLASH, the DC/DC shell temperature briefly exceeds the recommended working temperature when the load is 90%. Still, the whole power array does not have over-temperature protection. When the time increased to about 90 min, the temperature growth rate of shell temperature test point 2 gradually slowed and stabilized after 120 min. The main reason is that part of the DC/DC surface shell temperature exceeds the safe value range. MCU starts the fan to accelerate the speed of natural heat dissipation and conduction heat dissipation of the case surface. It can be seen that the effect of conduction heat dissipation is limited in a certain period. To optimize conduction heat dissipation, forced air cooling can reduce the case’s ambient temperature. Through high-temperature and high-load limit tests, the whole temperature of the electronic case is within the safe range. The structure and design of the closed automatic cooling case are reasonable and feasible.

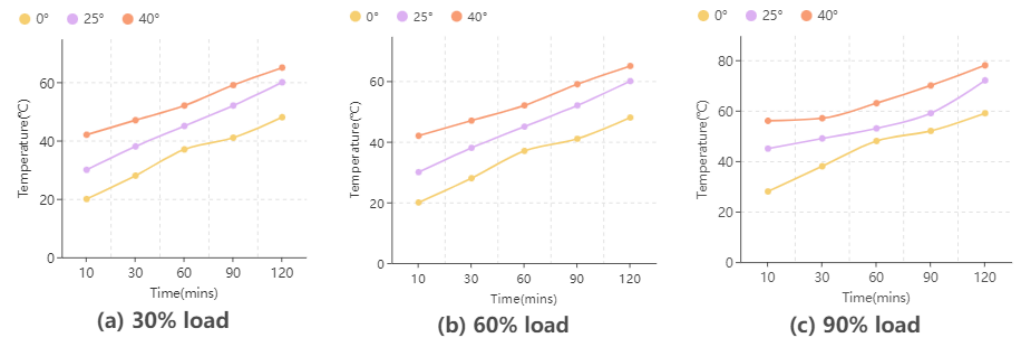


Figure 15. Temperature curve of shell temperature test point 2. (a) 30% load. (b) 60% load. (c) 90% load.

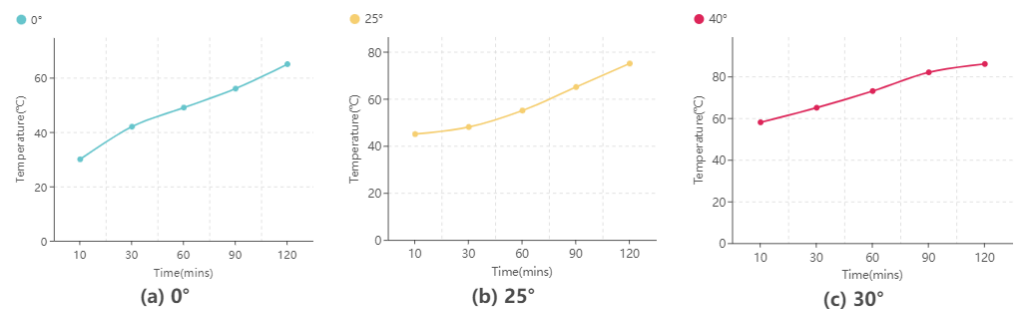


Figure 16. Shell temperature test point temperature curve of DCM3714 with 90% load (a) 0°. (b) 25°. (c) 30°.

From Table 5, the shell maximum temperature point 2 for two-hour tests reduces by 4.6–9.2% at different environmental temperatures. If ecological temperature increases, the cooling effect will weaken, but the shell temperature is still controlled within the safe limits.

Table 5. Highest shell temperature of test point 2 comparison diagram for two hours tests.

Environmental Temperature	Before Cooling	After Cooling	Percentage of Cooling
0°	72°	65°	9.2%
25°	81°	75°	8.0%
40°	90°	86°	4.6%

4.2. Comparison of Related Performance Parameters

The relevant performance parameters will be compared with the existing representative small mature cooling case and power modules to comprehensively evaluate the performance of the electronic case designed in this article. Peng developed the small signal processing case [22,23] as control group 1. The electronic case designed by Yu [6] served as control group 2. The electronic case designed by Li [3] served as control group 3. Table 6 lists the performance parameters of the electronic cooling case.

Firstly, it can be seen from Table 6 that, in control G1–G3, water cooling is not used in existing mature miniaturization case (module) designs, so reliability is defined as high. Secondly, temperature monitoring and control design are not adopted. If there is an issue with over-temperature, the power module may be destroyed. Thirdly, the design power of the whole system is limited below the watt level, the actual high power design is not realized, and the efficiency maximization test under the condition of high load output is not carried out. In addition, the electronic case (module) volume has been miniaturized, but the power density is far from the high power density design requirements. Heat dissipation cannot be fully reflected because of relatively low thermal power consumption. For example, control G3 did not use the case and only used a single module as a power source for testing and design. It only stayed in the test stage, with poor applicability. Finally, compared with control G1–G3, the electronic case with intelligent temperature control function and high reliability designed in this paper has passed the 90% load test, and the heat dissipation effect is noticeable. The output power of the whole system reaches 10,000 W level, and the load test power is 16 times control G3. The power density of the case with load is about ten times higher than control G1 and increases by 38% compared with the power density of the G3 with the bag. Therefore, the electronic case designed in this article has more performance advantages, such as intelligent control, high test power on load and overall design power, and tall case power density than the current cooling process.

Table 6. DC/DC series power supply information.

Case	Volume	Reliability	Intelligent Control	Test Power on Load	Overall Design Power	Case Power Density	Test Time
The Case	(28 × 23 × 15) cm ³	High	Yes	10,000 W	10,000 W	10 W/cm ³	2 h
G1	(42 × 26 × 29) cm ³	High	No	100 W	600 W	0.003 W/cm ³	2 h
G2	(22 × 16 × 50) cm ³	High	No	0 W	150 W	0 W/cm ³	2 h
G3	(11 × 56 × 12) cm ³	High	No	600 W	600 W	7.2 W/cm ³	2 h

5. Conclusions and Future Work

The wide application of miniaturized multi-board cases with high-power and high-density thermal design has become essential. However, most existing solutions stay in the thermal simulation stage, optimizing heat dissipation structure. There are no actual high-density designs and load high-power tests. In addition, intelligent monitoring and

temperature regulation measures are also not adopted. In this paper, a miniaturized and high-power density electronic case is designed. The power array is composed of DC/DC modules with high efficiency and the technology of parallel current equalization. Magnesium and aluminum alloy materials are used to consider the electronic case's surface strength and electromagnetic compatibility to enhance thermal conductivity. Heat dissipation mode accelerates conduction heat dissipation based on optimizing heat dissipation holes, adding fan groups to enhance heat exchange on the surface and inside of the conduction case. Automatic control modules are designed to form monitoring and feedback control mechanisms. The heat dissipation design of the miniaturized electronic case is proven to guarantee its regular operation after high temperature and high load environment tests. Compared with the mature miniaturized electronic case, the load power test is 16 times the current load power. When the heat dissipation effect is the same, the power density is about 10 times higher, and the performance is better.

The electronic case designed in this article is installed in a fixed and closed environment on land for testing. These system architectures, including features with confined space limitation (less than 10,000 cm³), high power output (more than 10,000 W), long working hours (more than 2 h), and variable output power (between 0–10,000 W), would benefit from this cooling configuration. For example, it could be used at high altitudes or in deep water high-speed moving environments. In that case, some DC/DC modules may fail to work due to changes caused by shock, vibration pressure, and temperature between internal and external heat dissipation channels, resulting in a decline in output power. The next step is to simulate a high altitude or deep water dynamic operating environment and test the electronic case with load to verify the effectiveness and reliability of the thermal design.

Author Contributions: Conceptualization, Z.C. and H.F.; methodology, Z.C. and C.Y.; software and data curation, Z.C.; validation and writing—original draft preparation, Z.C.; writing—review and editing, Z.C., H.F., and C.Y.; supervision, H.F. and G.Z. All authors have read and agreed to the published version of the manuscript.

Funding: This research was funded by the Luguang Yan Academician Workstation in YunNan Province (Project No.202305AF150049).

Data Availability Statement: Not applicable.

Acknowledgments: We would like to express our gratitude to Guoguang Zhang and Chong Yang for their meaningful support for this work.

Conflicts of Interest: The authors declare no conflict of interest.

References

1. Lv, Y. Research and Design of a Two-Channel High-Side Intelligent Power Switching Circuit. Master's Thesis, University of Electronic Science and Technology of China, Chengdu, China, 2022.
2. Ben, A.; Xie, P.; Huang, F.; Yu, H. Analysis and Design of Modular DC Power Cabinet Heat Dissipation in Substation. *Mach. Des. Manuf. Eng.* **2020**, *49*, 57–61.
3. Li, Y.; Li, Z.; Gao, L. Structural Thermal Design of a High Power Density Closed Power Supply. *Electro-Mech. Eng.* **2012**, *28*, 15–36.
4. Tan, H. Optimization Design and Simulation Analysis of Heat Dissipation of an Airborne Equipment Power Cabinet. *South China Agric. Mach.* **2015**, *52*, 138–140.
5. Yang, T. Structure and Heat Dissipation Analysis of Shipborne Water-cooled Cabinet. *Ship Electron. Countermeas.* **2022**, *45*, 106–110.
6. Yu, Q.; Ge, X. Heat Dissipation Optimization of High Power Supply Module. *Electron. World* **2021**, *8*, 170–171.
7. Fu, P.; Wen, W.; Li, Y. Research on Ventilation and Heat Dissipation Structure and Method of a New Energy Storage Power Supply. *Technol. Mark.* **2020**, *27*, 33–34.
8. Zhang, G.; Gao, Z.; Yang, L.; Zhang, C.; Design and Simulation Analysis of Heat Dissipation in Dense Arrangement of Multi-Switch Power Supply. *Road Mach. Constr. Mech.* **2020**, *37*, 85–89.
9. Huang, X.; Li, D.; Wei, H.; Hou, S. Optimization design of Heat Dissipation for High Power Microwave Power Supply. *Autom. Inf. Eng.* **2023**, *44*, 39–45.
10. Niu, Y.; Gan, F.; Gao, M.; Shi, J. Thermal resistance Model Establishment and Heat dissipation Design of DC/DC Power Module. *Power Electron. Technol.* **2021**, *55*, 137–140.
11. Zhou, Z.; Tang, H.; Yang, C.; Liu, L. Research on Improving the Working Life of Power Module. *Shanghai Electr. Technol.* **2014**, *7*, 14–17.

12. Li, X.; Cao, W.; Pei, Q. Thermal properties of AZ91D. *J. Henan Polytech. Univ.* **2010**, *29*, 685–688.
13. Xing, Y.; Xu, K.; Liu, Y.; Zhang, L.; Qi, C. Research progress of graphene's high thermal conductivity Mechanism and Heat Transfer Enhancement. *Chem. Eng.* **2015**, *29*, 54–60.
14. Yan, L.; Huang, H.; Li, S.; Qu, G. Research on the Standard and Application of Aviation Miniaturized Chassis. *Meas. Control Technol. Mag.* **2021**, *1*, 484–487.
15. Li, Z. Calculation Method and Optimization of Thermal Conductivity of Heat dissipation Hole in Printed Circuit Board. *Mod. Electron. Tech.* **2014**, *37*, 143–147.
16. Yu, G.; Li, F.; Tian, H. Design of ultra-thin Switching Power Supply with High Power Density. *Appl. Electron. Tech.* **2021**, *1*, 484–487.
17. Shuai, W. Design of Output Parallel Current Sharing Circuit. *Electron. Prod. World* **2023**, *30*, 95–97.
18. Yang, Y. Design of a temperature monitoring system based on single chip microcomputer and DS18B20. *J. Nonferrous Met. Des.* **2022**, *49*, 66–69.
19. Jiang, S.; Wang, B.; Yu, L.; Yu, T. Design and implementation of Multi-channel Data Sampling System Based on FPGA+AD7606. *Electron. Des. Eng.* **2022**, *30*, 103–107.
20. Yang, L. Analysis of Application Strategy of Relay in Automation Engineering. *Ind. Innov. Res.* **2023**, *2*, 154–156.
21. Xu, Y. An Intelligent Cooling System for Hydraulic Fan Motor. *Hydraul. Pneum. Seals* **2023**, *43*, 63–65.
22. Yang, A.; Yang, J.; Sun, B.; Yao, C. Modeling Design of Heat Dissipation Hole in Special Case Based on Icepak Analysis. *J. Mach. Des.* **2022**, *39*, 143–147.
23. Peng, H.; Hu, J.; Tao, G. Design of Heat Dissipation in Portable Miniaturized Signal Processing Case. *Electro-Mech. Eng.* **2020**, *36*, 18–21.

Disclaimer/Publisher's Note: The statements, opinions and data contained in all publications are solely those of the individual author(s) and contributor(s) and not of MDPI and/or the editor(s). MDPI and/or the editor(s) disclaim responsibility for any injury to people or property resulting from any ideas, methods, instructions or products referred to in the content.